Contribution from the Department of Inorganic Chemistry, Indian Association for the Cultivation of Science, Calcutta 700 032, India, and the Department of Chemistry and Laboratory for Molecular Structure and Bonding, Texas A&M University, College Station, Texas 77843

Trinucleation of Arylazo Oxime Ensembles. 2.[1] Linear $Fe^{II}Ni^{II}Fe^{II}$ and Related Systems

Samudranil Pal,[2a] Rabindranath Mukherjee,[2a] Milagros Tomas,[2b,c] Larry R. Falvello,[2b] and Animesh Chakravorty*[2a]

Received May 30, 1985

The tris(arylazo oximato)iron(II) anion, $Fe(RL)_3^-$, reacts smoothly with 3d metal(II) ions, affording heterometallic trinuclear species of type $M^{II}Fe^{II}_2(RL)_6$ (M = Mn, Co, Ni, Zn; HRL is RC(=NOH)N=NPh with R = Me, Ph). The structure of $NiFe_2(MeL)_6 \cdot CH_2Cl_2$ has been determined X-ray crystallographically. The complex belongs to the space group $P2_1/n$, with $Z = 4$. Unit cell dimensions are $a = 29.607$ (18) Å, $b = 19.732$ (11) Å, $c = 10.040$ (4) Å, $\beta = 90.53$ (4)°, and $V = 5865$ (5) Å^3. Refinement was achieved to $R = 0.0734$ and $R_w = 0.0933$. The trinuclear complex consists of two $Fe(MeL)_3^-$ segments coordinating the centrally placed nickel(II) ion with the help of six pendant oximato oxygen atoms. The NiO_6 octahedron thus produced is nearly regular. Within each $Fe(MeL)_3^-$ unit the three ligands (coordination at oxime and azo nitrogen atoms) are facially disposed. The FeN_6 coordination sphere is a trigonally compressed pseudooctahedron. The FeNiFe angle is 178.2 (1)°. The two $Fe(MeL)_3^-$ units within the same molecule have the same chirality ($\Delta\Delta$ or $\Lambda\Lambda$)—the crystal as a whole being racemic. The dichloromethane molecule is disordered in the crystal. All the trinuclear complexes display intense MLCT bands localized within the $Fe(RL)_3^-$ units at ~600 and ~400 nm. The M = Ni and Co species show ligand field transitions at ~1300 nm ($Dq \approx 760$ cm^{-1}). The powder EPR spectrum of $MnFe_2(MeL)_6$ ($S = {}^5/_2$) in pure form is closely similar to those of the same complex doped (1%) into $MFe_2(MeL)_6$ (M = Ni, Co, Zn). In all cases the dominant signal occurs at $g \approx 2$, showing that the zero-field splitting (and hence distortion of the MO_6 octahedron) is small as required by the X-ray structure of the M = Ni complex. The chromium(III) complex $[CrFe_2(MeL)_6]ClO_4 \cdot 2H_2O$ also reported here has a relatively large zero-field splitting ($D \approx 0.5$ cm^{-1}). In dichloromethane solution the quasi-reversible $M^{III}Fe_2(MeL)_6^+/M^{II}Fe_2(MeL)_6$ couples have the following E°_{298} values: M = Cr, -0.9 V (estimated); M = Mn, +0.51 V; M = Fe, +0.05 V; M = Co, +0.69 V; M = Ni, +1.3 V (estimated). In the trinuclear complexes the two bound $Fe(MeL)_3^-$ units undergo successive quasi-reversible 1e reductions, affording a pair of overlapping but clearly observable cyclic voltammetric couples in *all* cases. The pair, which expectedly shifts to higher potentials in going from a bivalent (e.g., E°_{298} for the M = Ni complex being -0.79 and -0.93 V) to a trivalent (E°_{298} for the M = Cr complex being -0.43 and -0.59 V) central metal ion, is diagnostic of trinucleation.

Introduction

This work pertains to the chemistry of a new class of linear trinuclear systems afforded by duplex ligation of an ensemble of six arylazo oxime donors,[1,3,4] RC(=NOH)N=NPh (HRL, R = Me, Ph). The first authentic example of this class is[1] the mixed-valence cation $Fe_3(RL)_6^+$, (**1**; details of only one ligand

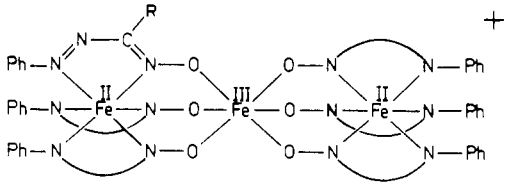

1

molecule are shown). The two $Fe(RL)_3^-$ moieties—each having an $Fe^{II}N_6$ coordination sphere—act as tridentate ligands through the oximato oxygen atoms. A central and bridging $Fe^{III}O_6$ polyhedron is thus produced. The aggregate $Fe^{II}Fe^{III}Fe^{II}$ is strictly linear,[1,5,6] and all the three metal polyhedra are pseudooctahedral.

We have undertaken a program to explore the applicability of the structural pattern **1** to other metal ions. As a first step in this endeavor, we examine here the synthesis and chemistry of heterometallic species in which only the central metal atom of **1** is selectively replaced by bivalent and trivalent 3d elements. While the chromium(III) complex $CrFe_2(MeL)_6^+$ is described, particular emphasis is given on the electrically neutral $Fe^{II}M^{II}Fe^{II}$ type, $MFe_2(RL)_6$. The X-ray structure of a representative system having the $Fe^{II}Ni^{II}Fe^{II}$ core has been determined. With use of this nickel(II) complex as a reference, the optical and EPR spectra of the various chelates are utilized for probing the stereochemical nature of the central MO_6 octahedra in the other complexes. Multiple sites of potential redox activity exist in the trinuclear aggregates: M, Fe, and RL. Electrochemical examination of such activity has revealed patterns of electron transfer that are diagnostic of trinucleation.

Results and Discussion

A. Synthesis by Trinuclear Reaggregation. A characteristic reaction of the $Fe_3(RL)_6^+$ cation is the selective and quantitative extrusion of the iron(III) atom by alkali resulting in the liberation of $Fe(RL)_3^-$ (eq 1). This anion, which can be isolated as sodium

$$Fe_3(RL)_6^+ + 3OH^- \rightarrow 2Fe(RL)_3^- + Fe(OH)_3 \quad (1)$$

$$2Fe(RL)_3^- + M^{2+} \rightarrow MFe_2(RL)_6 \quad (2)$$

or tetraphenylarsonium salts, has exclusive facial disposition of the three unsymmetrical bidentate chelate rings.[1,7] Addition of a bivalent metal perchlorate to the green ethanolic solution of $Fe(RL)_3^-$ leads to immediate darkening of color, and from the reaction mixture dark-colored complexes of composition $MFe_2(RL)_6$ (eq 2) are isolated in excellent yields with or without solvent of crystallization. We consider here the complexes having M = Mn, Co, Ni, and Zn. X-ray-quality crystals are difficult to grow in most cases. However, the solvate $NiFe_2(MeL)_6 \cdot CH_2Cl_2$, obtained from dichloromethane, afforded reasonable crystals and its structure was solved. The complex $CrFe_2(MeL)_6^+$ was synthesized (Cr^{3+} used instead of M^{2+} in eq 2) and isolated as a perchlorate salt. A similar use of Fe^{3+} in eq 2 leads to[1] reconstitution of $Fe_3(RL)_6^+$.

The synthetic reaction (2) can be reversed by addition of sodium hydroxide to acetone solutions of $MFe_2(RL)_6$. The central metal atom is selectively extruded (eq 3), liberating $M(OH)_2$ quantitatively. The solution is green due to $Fe(RL)_3^-$.

$$MFe_2(RL)_6 + 2OH^- \rightarrow 2Fe(RL)_3^- + M(OH)_2 \quad (3)$$

The various complexes and some physical data are listed in Table I. The complexes are generally soluble (solubility, R =

(1) Part 1: Pal, S.; Melton, T.; Mukherjee, R. N.; Chakravarty, A. R.; Tomas, M.; Falvello, L. R.; Chakravorty, A. *Inorg. Chem.* **1985**, *24*, 1250.
(2) (a) Indian Association for the Cultivation of Science. (b) Texas A&M University. (c) Permanent address: University of Zaragoza, Zaragoza, Spain.
(3) Ligands that as a single unit or as an ensemble bring about the situation in which two distinct redox centers are housed adjacently are called[1] duplex ligands.
(4) A fairly complete set of references on the coordination chemistry of arylazo oxime chelates can be found elsewhere.[1]
(5) Recently a linear $Fe^{II}Fe^{II}Fe^{II}$ system based on terminal aquo and bridging triazole ligands has been described.[6]
(6) Vos, G.; de Graff, R. A. G.; Haasnoot, J. G.; van der Kraan, A. M.; de Vaal, P.; Reedijk, J. *Inorg. Chem.* **1984**, *23*, 2905.
(7) Raghavendra, B. S. R.; Gupta, S.; Chakravorty, A. *Transition Met. Chem. (Weinheim, Ger.)* **1979**, *4*, 42.

0020-1669/86/1325-0200$01.50/0

Table I. Some Characterization Data

compd	IR data,[a] ν_{NO}, cm^{-1}	bulk susceptibility (298 K) μ_{eff}, μ_B	ligand field transition[b] λ_{max}, nm (ϵ, M^{-1} cm^{-1})
$NiFe_2(MeL)_6 \cdot CH_2Cl_2$	1245	3.10	1333 (67)
$NiFe_2(MeL)_6 \cdot 2H_2O$	1245	3.16	1330 (70)
$NiFe_2(PhL)_6$	1255	3.55	1300[c] (50)
$CoFe_2(MeL)_6 \cdot 2H_2O$	1245	4.98	1350 (55)
$CoFe_2(PhL)_6$	1260	5.02	1325 (90)
$MnFe_2(MeL)_6 \cdot 2H_2O$	1240	6.00	
$MnFe_2(PhL)_6$	1250	5.78	
$ZnFe_2(MeL)_6 \cdot 2H_2O$	1260	*d*	
$ZnFe_2(PhL)_6$	1275	*d*	
$CrFe_2(MeL)_6ClO_4 \cdot 2H_2O$	1245	3.80	

[a] In KBr disk (4000–300 cm^{-1}); ν_{NO} is broad and strong. [b] Solvent is chloroform. [c] Shoulder. [d] Diamagnetic.

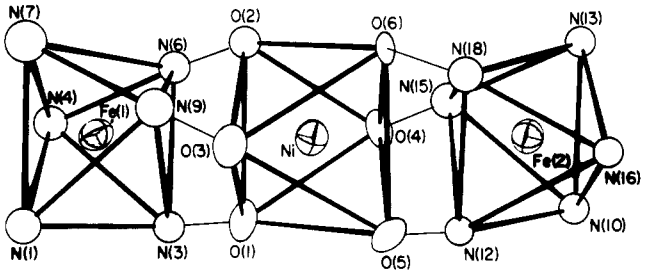

Figure 1. Plot of the coordination polyhedra about the iron and nickel atoms. All atoms are represented by their 40% probability ellipsoids.

Me > R = Ph) in polar organic solvents, affording brownish green to bluish green solutions. All species display a strong N–O stretch at ~1250 cm^{-1} characteristic[8-11] of chelated arylazo oximes. While the $M^{II}Fe_2(RL)_6$ species are generally nonelectrolytic in polar solvents, the chromium(III) complex acts as a 1:1 electrolyte (Λ_M = 150 Ω^{-1} cm^2 mol^{-1}) in acetonitrile solution.

B. X-ray Structure of $NiFe_2(MeL)_6 \cdot CH_2Cl_2$. The asymmetric unit of the crystal comprises one molecule of the neutral complex $NiFe_2(MeL)_6$ along with partially occupied sites containing CH_2Cl_2 molecules. All atoms are on general equivalent positions in the space group $P2_1/n$. The trinuclear complex indeed belongs to the gross structural type **1**. It consists of two $Fe(MeL)_3^-$ fragments coordinating the centrally placed nickel(II) ion. Figure 1 shows the coordination polyhedra about the three metal atom centers. Parts a and b of Figure 2 show the structures and atom-labeling schemes for the groups coordinated to the two iron atoms, designated Fe(1) and Fe(2). Selected bond distances and angles are in Tables II and III, respectively.

The central nickel atom is octahedrally bonded by six oximato oxygen atoms pendant from the two $Fe(MeL)_3^-$ fragments. The octahedron is not exactly regular but is nearly so with an average[12] Ni–O distance of 2.056 [7] Å and average cis O–Ni–O bond angle of 90.0 [5]°. In salt hydrates having the $Ni(H_2O)_6^{2+}$ ion the NiO_6 sphere is[13] invariably a slightly distorted octahedron and the average Ni–O bond length, like that in $NiFe_2(MeL)_6 \cdot CH_2Cl_2$, lies very close to 2.06 Å. The same applies[14] to $[Ni(pyO)_6](BF_4)_2$ (pyO = pyridine *N*-oxide).

The average chelate bite angle on the two iron centers is 78.8 [5]°. The large negative deviation of the bite angle from 90° *necessarily* implies the presence of substantial trigonal compression. Indeed the two iron centers can be considered to have distorted-trigonal-antiprismatic coordination. The distortions from octahedral geometry can be conceptalized, for each iron center, as being the result of trigonal compression along the Fe···Ni vector, followed by an isotropic contraction of the triangular face which abuts a triangular face of the nickel coordination octahedron. Thus, for the coordination polyhedron about Fe(1), the average edge length of the triangle defined by atoms N(3), N(6), and N(9) is 2.67 [3] Å, while that of the terminal face (N(1), N(4), and N(7)) is 2.86 [5] Å. Similarly considering the atoms coordinated to Fe(2), the triangle formed by atoms N(12), N(15), and N(18) has an average edge of 2.68 [3] Å, while the terminal triangle (N(10), N(13), and N(16)) has an average edge length of 2.92 [6] Å. As noted above, triangular faces of the terminal iron coordination polyhedra abut triangular faces of the central octahedron of oxygen atoms about nickel. The abutting faces are not eclipsed, however, and the average torsion angle O–Ni–Fe–N, involving terminal O and N atoms which are chemically bonded to each other, is 18.6 [6]°.

At each iron atom the three chelate rings are facially disposed, and this is necessary for the ligation of the pendant oxygen atoms to the central nickel. The chelate rings are planar. At the Fe(1) end, the angle between the plane containing N(1) and that containing N(4) is 102°; the dihedral angle between the ligand plane containing N(1) and that with N(7) is 72°; for the planes containing N(4) and N(7), respectively, the dihedral angle is 97°. At the Fe(2) end of the molecule, the angle between the plane of the ligand containing N(10) and that of the ligand containing N(13) is 85°, for the planes containing N(10) and N(16) the corresponding angle is 77°, and for the planes containing N(13) and N(16) it is 79°. The dimensions of the chelate ring in the present complex are comparable to those in other transition-metal complexes of arylazo oximes.[1,15-18] The average N=N and N—O distances are respectively 1.29 [1] and 1.31 [1] Å. The average Fe–N(O) (1.92 [1] Å) and Fe–N(Ph) (1.94 [1] Å) distances are comparable to those found[1] in $Fe_3(PhL)_6^+$.

The $Fe_3(PhL)_6^+$ cation is centrosymmetric with strictly linear arrangement of the $Fe^{II}Fe^{III}Fe^{II}$ chain, and the two $Fe(PhL)_3^-$ units necessarily have opposite chirality (Δ, Λ), making $Fe_3(PhL)_6^+$ achiral. The arrangement in $NiFe_2(MeL)_6$ differs in a subtle and significant way. The Ni···Fe(1) and Ni···Fe(2) distances are respectively 3.486 (5) and 3.475 (5) Å, and the Fe(1)···Ni···Fe(2) angle is 178.2 (1)°. The metal chain is nearly but not exactly linear. For a given molecule in the crystal, both tris-chelated iron centers have the same stereochemical conformation. Thus each molecule is chiral. The drawings in Figure 2 and the coordinates listed later in Table VII represent a molecule in a Δ,Δ conformation. The crystal as a whole is, however, racemic.

In view of the definitive structural results obtained earlier[1] for $Fe_3(PhL)_6^+$ (central metal ion trivalent) and reported now for $NiFe_2(MeL)_6$ (central metal ion bivalent), it is inferred that all the complexes described in this paper belong to the same gross structural type. Strong support to this inference is provided by optical and EPR spectra as well by electrochemical data.

C. Optical Spectra: Ligand Field Bands of the MO_6 Core. The complexes reported here display intense absorption bands (Figure 3) at ~600 and ~400 nm due to Fe–(azo–imine) charge transfer

(8) Kalia, K. C.; Chakravorty, A. *Inorg. Chem.* **1969**, *8*, 2586.
(9) Bandyopadhyay, P.; Mascharak, P. K.; Chakravorty, A. *J. Chem. Soc., Dalton Trans.* **1981**, 623.
(10) Chakravarty, A. R.; Chakravorty, A. *Inorg. Chem.* **1981**, *20*, 3138.
(11) Bandyopadhyay, P.; Mascharak, P. K.; Chakravorty, A. *J. Chem. Soc., Dalton Trans.* **1982**, 675.
(12) The deviation in brackets is calculated as

$$[\sum_{i=1}^{n} \Delta_i^2/n(n-1)]^{1/2}$$

where Δ_i is the deviation of the *i*th value from the mean of *n* values.
(13) Ray, S.; Zalkin, A.; Templeton, D. H. *Acta Crystallogr., Sect. B: Struct. Crystallogr. Cryst. Chem.* **1973**, *B29*, 2741. Montgomery, H.; Lingafelter, E. C. *Acta Crystallogr.* **1964**, *17*, 1478. Montgomery, H. *Acta Crystallogr., Sect. B: Struct. Crystallogr. Cryst. Chem.* **1979**, *B35*, 155. Montgomery, H. *Acta Crystallogr., Sect. B: Struct. Crystallogr. Cryst. Chem.* **1980**, *B36*, 440. Shchegoleva, T. M.; Iskhakova, L. D.; Ovanesyan, S. M.; Shakhnazaryan, A. A.; Trunov, V. K. *Russ. J. Inorg. Chem. (Engl. Transl.)* **1983**, *28*, 1286.
(14) van Ingen Schenau, A. D.; Verschoor, G. C.; Romers, C. *Acta Crystallogr., Sect. B: Struct. Crystallogr. Cryst. Chem.* **1974**, *B30*, 1686.
(15) Bandyopadhyay, D.; Bandyopadhyay, P.; Chakravorty, A.; Cotton, F. A.; Falvello, L. R. *Inorg. Chem.* **1984**, *23*, 1785.
(16) Bandyopadhyay, D.; Bandyopadhyay, P.; Chakravorty, A.; Cotton, F. A.; Falvello, L. R. *Inorg. Chem.* **1983**, *22*, 1315.
(17) Dickman, M. H.; Doedens, R. J. *Inorg. Chem.* **1980**, *19*, 3112. Pal, S.; Bandyopadhyay, D.; Datta, D.; Chakravorty, A. *J. Chem. Soc., Dalton Trans.* **1985**, 159.
(18) Chakravarty, A. R.; Chakravorty, A.; Cotton, F. A.; Falvello, L. R.; Ghosh, B. K.; Tomas, M. *Inorg. Chem.* **1983**, *22*, 1892.

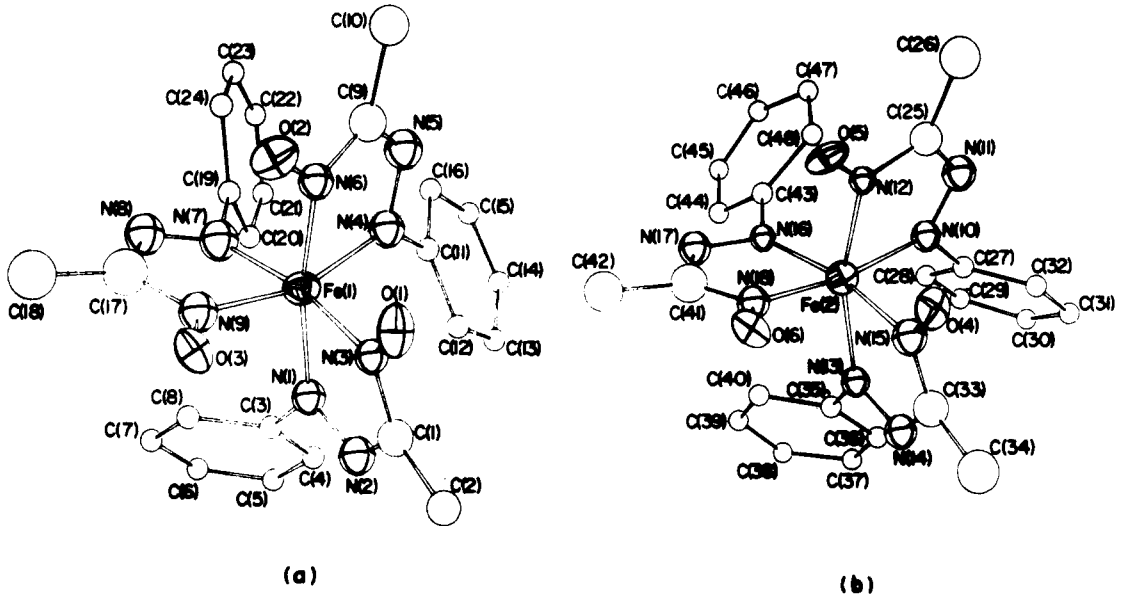

Figure 2. ORTEP plot and labeling scheme for the ligands coordinated to (a) Fe(1) and (b) Fe(2). Phenyl-group carbon atoms are shown as small circles, for clarity. All other atoms are represented at the 40% probability level.

Table II. Important Distances (Å) and Their Estimated Standard Deviations[a] for $NiFe_2(MeL)_6 \cdot CH_2Cl_2$

Ni···Fe(1)	3.486 (5)	O(4)–N(15)	1.29 (2)	N(16)–N(17)	1.30 (2)
Ni···Fe(2)	3.475 (5)	O(5)–N(12)	1.292 (15)	N(16)–C(43)	1.43 (2)
Ni–O(1)	2.053 (13)	O(6)–N(18)	1.30 (2)	N(17)–C(41)	1.37 (2)
Ni–O(2)	2.049 (12)	N(1)–N(2)	1.31 (2)	N(18)–C(41)	1.28 (2)
Ni–O(3)	2.079 (11)	N(1)–C(3)	1.46 (2)	C(1)–C(2)	1.46 (2)
Ni–O(4)	2.030 (12)	N(2)–C(1)	1.34 (2)	C(3)–C(4)	1.34 (3)
Ni–O(5)	2.072 (11)	N(3)–C(1)	1.33 (2)	C(3)–C(8)	1.42 (3)
Ni–O(6)	2.052 (11)	N(4)–N(5)	1.31 (2)	C(9)–C(10)	1.53 (2)
Fe(1)–N(1)	1.925 (14)	N(4)–C(11)	1.49 (2)	C(11)–C(12)	1.38 (2)
Fe(1)–N(3)	1.933 (14)	N(5)–C(9)	1.37 (2)	C(11)–C(16)	1.40 (2)
Fe(1)–N(4)	1.95 (2)	N(6)–C(9)	1.30 (2)	C(17)–C(18)	1.52 (3)
Fe(1)–N(6)	1.899 (15)	N(7)–(8)	1.27 (2)	C(19)–C(20)	1.36 (3)
Fe(1)–N(7)	1.91 (2)	N(7)–C(19)	1.50 (2)	C(19)–C(24)	1.43 (3)
Fe(1)–N(9)	1.92 (2)	N(8)–C(17)	1.35 (2)	C(25)–C(26)	1.53 (3)
Fe(2)–N(10)	1.914 (13)	N(9)–C(17)	1.38 (2)	C(27)–C(28)	1.42 (2)
Fe(2)–N(12)	1.903 (14)	N(10)–N(11)	1.29 (2)	C(27)–C(32)	1.39 (2)
Fe(2)–N(13)	2.000 (15)	N(10)–C(27)	1.43 (2)	C(33)–C(34)	1.50 (3)
Fe(2)–N(15)	1.95 (2)	N(11)–C(25)	1.40 (2)	C(35)—C(36)	1.37 (2)
Fe(2)–N(16)	1.938 (14)	N(12)–C(25)	1.34 (2)	C(35)–C(40)	1.41 (3)
Fe(2)–N(18)	1.902 (14)	N(13)–N(14)	1.26 (2)	C(41)–C(42)	1.55 (3)
O(1)–N(3)	1.30 (2)	N(13)–C(35)	1.45 (2)	C(43)–C(44)	1.33 (2)
O(2)–N(6)	1.33 (2)	N(14)–C(33)	1.32 (2)	C(43)–C(48)	1.42 (3)
O(3)–N(9)	1.32 (2)	N(15)–C(33)	1.31 (2)		

[a] Numbers in parentheses are estimated standard deviations in the least significant digits.

within the $Fe(RL)_3^-$ units as in the case[1] of $Fe_3(RL)_6^+$. This vitiates the observation of ligand field transitions within the central MO_6 polyhedron except for the first transition in the cases of M = Ni and Co. The $NiFe_2(RL)_6$ species display a broad (width at half-height, $\omega_{1/2}$, ~800 cm^{-1}) and relatively weak Gaussian-shaped band at ~1300 nm (Table I; Figure 3). Assigning this to the idealized $^3A_2 \rightarrow {}^3T_2$ transition, one obtains $Dq \approx 760$ cm^{-1}. The ligand field strength of the six oximato oxygen atoms in $NiFe_2(RL)_6$ is thus weaker than that of six aquo oxygen atoms in $Ni(H_2O)_6^{2+}$ (Dq = 850 cm^{-1}).[19] The energy of the $^4T_1 \rightarrow {}^4T_2$ transition in $Co(H_2O)_6^{2+}$ is slightly lower[19] than that of $^3A_2 \rightarrow {}^3T_2$ in $Ni(H_2O)_6^{2+}$. A corresponding relationship exists between $NiFe_2(RL)_6$ and $CoFe_2(RL)_6$—the latter showing the $^4T_1 \rightarrow {}^4T_2$ transition ($\omega_{1/2} \approx 1000$ cm^{-1}) of the CoO_6 core at ~1350 nm (Table I and Figure 3).

D. EPR Spectra of the MO_6 Core. Since the $Fe(RL)_3^-$ moiety is[1,7] low spin ($S = 0$), the observed bulk magnetic moments (Table I) of the trinuclear species reflect the spin character of the central MO_6 polyhedron: M = Cr^{III}, $S = {}^3/_2$; M = Mn^{II}, $S = {}^5/_2$; M = Co^{II}, $S = {}^3/_2$; M = Ni^{II}, $S = 1$; M = Zn^{II}, $S = 0$.

EPR spectra were examined at X-band for powdered samples of pure and doped (1%) complexes at room temperature (~298 K) and at 77 K. The nickel(II) and cobalt(II) complexes are EPR-silent, evidently due to rapid relaxation. These as well as the zinc(II) complexes were used as host lattices for doping manganese(II), which was used as a probe[20] for stereochemical characterization of the MO_6 polyhedron. The doped complexes are designated as $M(Mn)Fe_2(RL)_6$.

Results are in Figure 4 and Table IV. In all cases the dominant feature is a strong resonance at $g \approx 2$ with several weak resonances at lower and higher fields. The MnO_6 octahedron is thus[21] nearly regular with very small zero-field splitting. The spectra of the polycrystalline samples[22] change little on going from room tem-

(19) Sutton, D. "Electronic Spectra of Transition Metal Complexes"; McGraw-Hill: London, 1968; pp 147–148.

(20) Birdy, R. B.; Goodgame, M. *J. Chem. Soc., Dalton Trans.* **1983**, 1469.

(21) Dowsing, R. D.; Gibson, J. F.; Goodgame, M.; Hayward, P. J. *J. Chem. Soc. A* **1969**, 187.

(22) In 1:1 MeCN–toluene glass (77 K) $MnFe_2(MeL)_6$ shows a strong hyperfine split resonance at 3300 G along with weak resonances at 4400, 2400, 1360, and 680 G.

Table III. Important Angles (deg) and Their Estimated Standard Deviations[a] for $NiFe_2(MeL)_6 \cdot CH_2Cl_2$

Fe(1)···Ni···Fe(2)	178.2 (1)	Ni···Fe(2)–N(15)	54.1 (5)	Fe(2)–N(13)–N(14)	118 (1)
Fe(1)···Ni–O(1)	55.8 (4)	Ni···Fe(2)–N(16)	120.5 (5)	Fe(2)–N(13)–C(35)	131 (1)
Fe(1)···Ni–O(2)	56.1 (4)	Ni···Fe(2)–N(18)	54.0 (6)	N(14)–N(13)–C(35)	110 (2)
Fe(1)···Ni–O(3)	55.5 (4)	N(10)–Fe(2)–N(12)	79.6 (6)	N(13)–N(14)–C(33)	112 (2)
Fe(1)···Ni–O(4)	123.1 (4)	N(10)–Fe(2)–N(13)	91.8 (6)	Fe(2)–N(15)–O(4)	123 (1)
Fe(1)···Ni–O(5)	126.7 (4)	N(10)–Fe(2)–N(15)	93.3 (6)	Fe(2)–N(15)–C(33)	114 (2)
Fe(1)···Ni–O(6)	124.2 (4)	N(10)–Fe(2)–N(16)	99.4 (6)	O(4)–N(15)–C(33)	123 (2)
Fe(2)···Ni–O(1)	124.1 (4)	N(10)–Fe(2)–N(18)	169.5 (6)	Fe(2)–N(16)–N(17)	115 (1)
Fe(2)···Ni–O(2)	122.4 (4)	N(12)–Fe(2)–N(13)	161.4 (6)	Fe(2)–N(16)–C(43)	135 (1)
Fe(2)···Ni–O(3)	126.1 (4)	N(12)–Fe(2)–N(15)	87.9 (7)	N(17)–N(16)–C(43)	110 (2)
Fe(2)···Ni–O(4)	55.3 (4)	N(12)–Fe(2)–N(16)	97.6 (6)	N(16)–N(17)–C(41)	113 (2)
Fe(2)···Ni–O(5)	54.8 (4)	N(12)–Fe(2)–N(18)	90.2 (6)	Fe(2)–N(18)–O(6)	127 (1)
Fe(2)···Ni–O(6)	55.9 (4)	N(13)–Fe(2)–N(15)	76.2 (7)	Fe(2)–N(18)–C(41)	114 (1)
O(1)–Ni–O(2)	93.3 (5)	N(13)–Fe(2)–N(16)	100.0 (6)	O(6)–N(18)–C(41)	118 (2)
O(1)–Ni–O(3)	90.7 (5)	N(13)–Fe(2)–N(18)	98.6 (6)	N(2)–C(1)–N(3)	113 (2)
O(1)–Ni–O(4)	88.7 (5)	N(15)–Fe(2)–N(16)	166.9 (6)	N(2)–C(1)–C(2)	123 (2)
O(1)–Ni–O(5)	89.4 (5)	N(15)–Fe(2)–N(18)	88.4 (7)	N(3)–C(1)–C(2)	123 (2)
O(1)–Ni–O(6)	179.7 (9)	N(16)–Fe(2)–N(18)	79.7 (7)	N(1)–C(3)–C(4)	121 (2)
O(2)–Ni–O(3)	90.4 (5)	Ni–O(1)–N(3)	112 (1)	N(1)–C(3)–C(8)	113 (2)
O(2)–Ni–O(4)	88.2 (5)	Ni–O(2)–N(6)	110 (1)	C(4)–C(3)–C(8)	126 (2)
O(2)–Ni–O(5)	177.0 (6)	Ni–O(3)–N(9)	110 (1)	N(5)–C(9)–N(6)	116 (2)
O(2)–Ni–O(6)	87.0 (5)	Ni–O(4)–N(15)	114 (1)	N(5)–C(9)–C(10)	120 (2)
O(3)–Ni–O(4)	178.5 (5)	Ni–O(5)–N(12)	110.7 (9)	N(6)–C(9)–C(10)	124 (2)
O(3)–Ni–O(5)	90.9 (5)	Ni–O(6)–N(18)	112 (1)	N(4)–C(11)–C(12)	115 (2)
O(3)–Ni–O(6)	89.0 (5)	Fe(1)–N(1)–N(2)	115 (1)	N(4)–C(11)–C(16)	117 (2)
O(4)–Ni–O(5)	90.5 (5)	Fe(1)–N(1)–C(3)	133 (1)	C(12)–C(11)–C(16)	127 (2)
O(4)–Ni–O(6)	91.6 (5)	N(2)–N(1)–C(3)	112 (1)	N(8)–C(17)–N(9)	112 (2)
O(5)–Ni–O(6)	90.4 (5)	N(1)–N(2)–C(1)	117 (2)	N(8)–C(17)–C(18)	126 (2)
Ni···Fe(1)–N(1)	120.4 (5)	Fe(1)–N(3)–O(1)	125 (1)	N(9)–C(17)–C(18)	121 (2)
Ni···Fe(1)–N(3)	53.9 (5)	Fe(1)–N(3)–C(1)	116 (1)	N(7)–C(19)–C(20)	115 (2)
Ni···Fe(1)–N(4)	122.5 (5)	O(1)–N(3)–C(1)	119 (1)	N(7)–C(19)–C(24)	113 (2)
Ni···Fe(1)–N(6)	53.3 (5)	Fe(1)–N(4)–N(5)	114 (1)	C(20)–C(19)–C(24)	132 (2)
Ni···Fe(1)–N(7)	120.2 (6)	Fe(1)–N(4)–C(11)	134 (1)	N(11)–C(25)–N(12)	114 (2)
Ni···Fe(1)–N(9)	53.7 (5)	N(5)–N(4)–C(11)	111 (2)	N(11)–C(25)–C(26)	121 (2)
N(1)–Fe(1)–N(3)	79.0 (6)	N(4)–N(5)–C(9)	114 (2)	N(12)–C(25)–C(26)	125 (2)
N(1)–Fe(1)–N(4)	98.6 (7)	Fe(1)–N(6)–O(2)	127 (1)	N(10)–C(27)–C(28)	119 (2)
N(1)–Fe(1)–N(6)	167.6 (6)	Fe(1)–N(6)–C(9)	116 (1)	N(10)–C(27)–C(32)	121 (2)
N(1)–Fe(1)–N(7)	97.6 (6)	O(2)–N(6)–C(9)	117 (2)	C(28)–C(27)–C(32)	120 (2)
N(1)–Fe(1)–N(9)	97.7 (7)	Fe(1)–N(7)–N(8)	117 (1)	N(14)–C(33)–N(15)	120 (2)
N(3)–Fe(1)–N(4)	101.4 (6)	Fe(1)–N(7)–C(19)	130 (2)	N(14)–C(33)–C(34)	119 (2)
N(3)–Fe(1)–N(6)	89.3 (6)	N(8)–N(7)–C(19)	110 (2)	N(15)–C(33)–C(34)	121 (2)
N(3)–Fe(1)–N(7)	167.4 (7)	N(7)–N(8)–C(17)	116 (2)	N(13)–C(35)–C(36)	121 (2)
N(3)–Fe(1)–N(9)	89.7 (7)	Fe(1)–N(9)–O(3)	124 (1)	N(13)–C(35)–C(40)	116 (2)
N(4)–Fe(1)–N(6)	79.4 (7)	Fe(1)–N(9)–C(17)	115 (2)	C(36)–C(35)–C(40)	123 (2)
N(4)–Fe(1)–N(7)	91.2 (7)	O(3)–N(9)–C(17)	119 (2)	N(17)–C(41)–N(18)	118 (2)
N(4)–Fe(1)–N(9)	161.8 (7)	Fe(2)–N(10)–N(11)	118 (1)	N(17)–C(41)–C(42)	117 (2)
N(6)–Fe(1)–N(7)	94.7 (6)	Fe(2)–N(10)–C(27)	131 (1)	N(18)–C(41)–C(42)	125 (2)
N(6)–Fe(1)–N(9)	86.3 (7)	N(11)–N(10)–C(27)	110 (1)	N(16)–C(43)–C(44)	118 (2)
N(7)–Fe(1)–N(9)	78.7 (7)	N(10)–N(11)–C(25)	112 (2)	N(16)–C(43)–C(48)	117 (2)
Ni···Fe(2)–N(10)	119.5 (6)	Fe(2)–N(12)–O(5)	124 (1)	C(44)–C(43)–C(48)	125 (2)
Ni···Fe(2)–N(12)	53.6 (5)	Fe(2)–N(12)–C(25)	115 (1)		
Ni···Fe(2)–N(13)	120.0 (5)	O(5)–N(12)–C(25)	119 (2)		

[a] Numbers in parentheses are estimated standard deviations in the least significant digits.

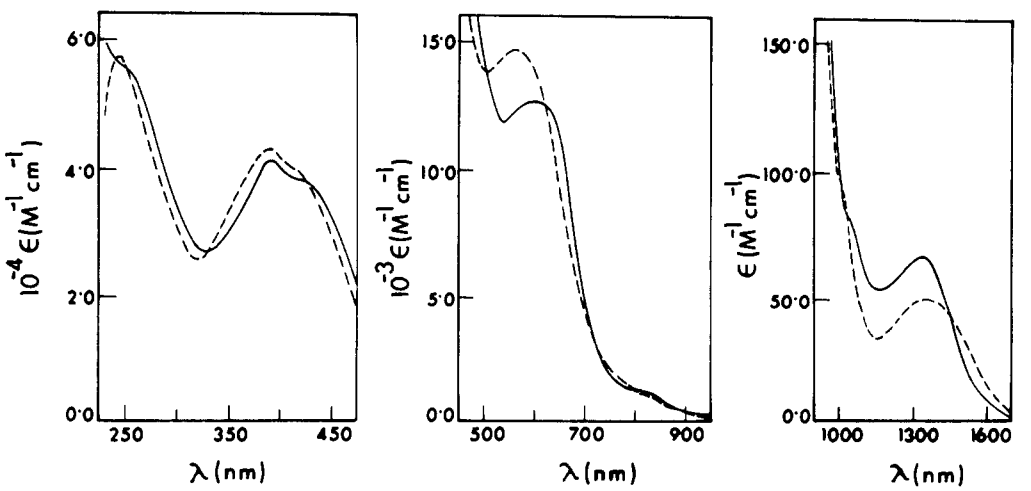

Figure 3. Electronic spectra of $NiFe_2(MeL)_6 \cdot CH_2Cl_2$ (—) and $CoFe_2(MeL)_6 \cdot 2H_2O$ (- - -) in chloroform.

Table IV. X-Band EPR Spectral Data[a] in the Polycrystalline Phase

compd	temp, K	*H*, G
$MnFe_2(MeL)_6 \cdot 2H_2O$[b]	298	1600, 2600, 3320,[c] 4200
	77	1600, 2600, 3360,[c] 4200
$Ni(Mn)Fe_2(MeL)_6 \cdot CH_2Cl_2$[d,e]	298	1600, 2600, 3320,[c] 4200
	77	1560, 2600, 3340,[c] 4240
$[CrFe_2(MeL)_6]ClO_4 \cdot 2H_2O$	298, 77[f]	1000, 1320, 1800,[c] 3200, 3340

[a] Measurements are made at microwave frequency 9.13 GHz. [b] Two extremely weak resonances occur at 560 and 1000 G. [c] Very strong signal; all other resonances are weak. [d] Doping is done to the extent of 1% by cocrystallization from dichloromethane. [e] The corresponding Co(Mn) and Zn(Mn) species have virtually identical (±20 G) resonance positions, which therefore are not tabulated separately. [f] In acetonitrile–toluene (1:1) frozen solution (77 K) resonance positions are almost the same (±20 G).

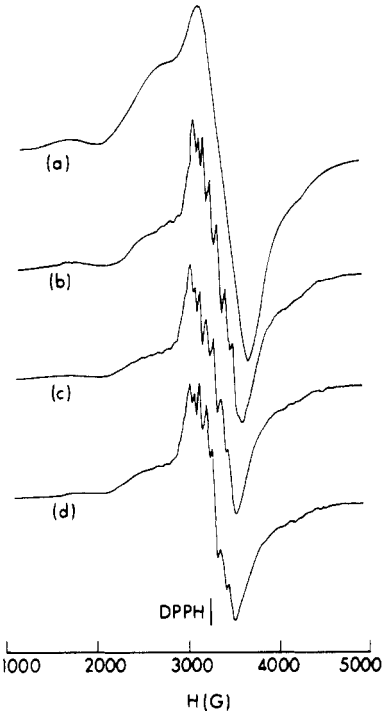

Figure 4. X-Band EPR spectra of polycrystalline pure and doped $MnFe_2(MeL)_6$ (298 K): (a) pure; (b) Ni(Mn); (c) Co(Mn); (d) Zn(Mn).

perature to 77 K. The crucial result is that the spectrum of $Ni(Mn)Fe_2(MeL)_6$ is very closely similar[23] to that of the pure manganese(II) complex. The inherent geometry of the MnO_6 polyhedron in the pure complex is thus essentially the same as that of the X-ray-characterized NiO_6 polyhedron. Such correlation extends further—the EPR spectra of all $M(Mn)Fe_2(MeL)_6$ (M = Mn, Co, Ni, Zn) species are alike and the pure complexes therefore have very similar MO_6 octahedra.[24] The doped complexes show ^{55}Mn hyperfine structure, which is absent in the case of the pure manganese(II) complex. This shows that, in the doped species, the molecules of the manganese(II) complex occur within the host lattice and do not form a separate phase, which would have afforded a spectrum without hyperfine structure like that of the pure manganese(II) complex.

The EPR spectra of $[CrFe_2(MeL)_6]ClO_4 \cdot 2H_2O$ in powder and frozen solution consist of a very strong feature at $g = 3.70$ with a weak resonance at $g \approx 2$. Some other very weak signals also occur above $g = 4$ (Table IV). Such spectra are characteristic[25] of large zero-field splitting, $2D >> h\nu$ ($h\nu = 0.31$ cm^{-1} at X-band). With use of the approximate equation (4),[26] where g is the experimental g value of the strong signal, D is estimated to be ~ 0.5 cm^{-1}. The implication of the EPR result is that the chromium(III) (d^3) complex is electronically more distorted than the corresponding manganese(II) (d^5) complex.

$$g = 4[1 - 3\beta^2H^2/4D^2] \quad (4)$$

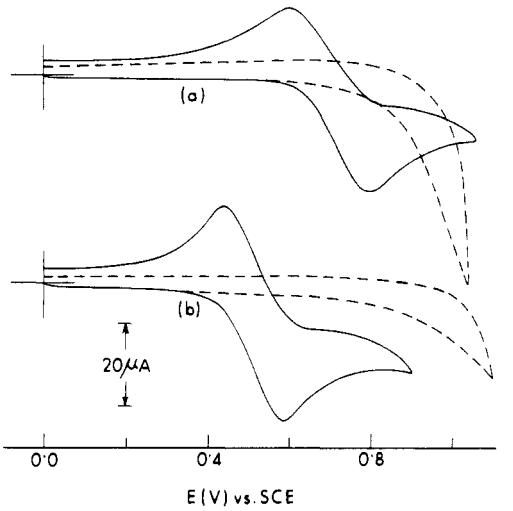

Figure 5. Cyclic voltammograms (scan rate 50 mV s^{-1}) of $\sim 10^{-3}$ M solutions of (a) $CoFe_2(MeL)_6 \cdot 2H_2O$ (—) and $ZnFe_2(MeL)_6 \cdot 2H_2O$ (---) and (b) $MnFe_2(MeL)_6 \cdot 2H_2O$ (—) and $NiFe_2(MeL)_6 \cdot 2H_2O$ (---) in dichloromethane (0.1 M TEAP) at a platinum electrode (298 K).

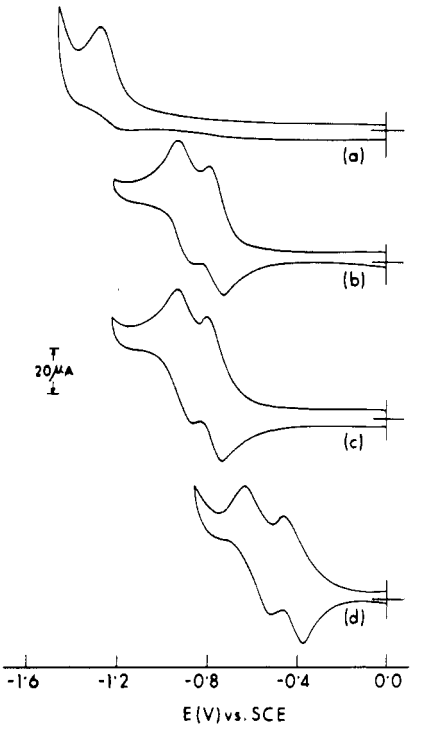

Figure 6. Cyclic voltammograms (scan rate 50 mV s^{-1}) of $\sim 10^{-3}$ M solutions of (a) $NaFe(MeL)_3 \cdot H_2O$, (b) $MnFe_2(MeL)_6 \cdot 2H_2O$, (c) $NiFe_2(MeL)_6 \cdot 2H_2O$, and (d) $[CrFe_2(MeL)_6]ClO_4 \cdot 2H_2O$ in acetonitrile (0.1 M TEAP) at a platinum electrode (298 K).

(23) This similarity indicates that nickel(II)–manganese(II) spin–spin interaction is negligibly small. The same comment applies to the manganese(II)–cobalt(II) interaction in $Co(Mn)Fe_2(MeL)_6$, which displays EPR signals for the manganese(II) center only (see text).

(24) The EPR spectra of $M(Mn)Fe_2(PhL)_6$ (M = Mn, Co, Ni, Zn) were also examined. Again a strong $g \approx 2$ signal is observed flanked by weak resonances on either side.

(25) Singer, L. S. *J. Chem. Phys.* **1955**, *23*, 379. Hempel, J. C.; Morgan, L. O.; Lewis, W. B. *Inorg. Chem.* **1970**, *9*, 2064. Pedersen, E.; Toftlund, H. *Inorg. Chem.* **1974**, *13*, 1603.

(26) Richens, D. T.; Sawyer, D. T. *J. Am. Chem. Soc.* **1979**, *101*, 3681. Ferrante, R. F.; Wilkerson, J. L.; Graham, W. R. M.; Weltner, W. *J. Chem. Phys.* **1977**, *67*, 5904.

Table V. Electrochemical[a,b] Data at 298 K

compd	$E°_{298}$, V (ΔE_p, mV)[c]	n (E, V)[d,e]	$-E°_{298}$, V (ΔE_p, mV)[f]
$NiFe_2(MeL)_6 \cdot CH_2Cl_2$	*g*	*h*	0.85 (70), 1.00 (70)
$NiFe_2(MeL)_6 \cdot 2H_2O$	*g*	*h*	0.86 (70), 1.01 (70)
$MnFe_2(MeL)_6 \cdot 2H_2O$	0.51 (140)	1.07 (0.8)	0.85 (60), 0.99 (60)
$MnFe_2(PhL)_6$	0.56 (110)	1.01 (0.8)	*i*
$CoFe_2(MeL)_6 \cdot 2H_2O$	0.69 (180)	0.96 (1.0)	0.84 (80), 0.98 (90)
$CoFe_2(PhL)_6$	0.72 (140)	0.99 (1.0)	*i*
$ZnFe_2(MeL)_6 \cdot 2H_2O$	*g*	*h*	0.76 (120), 0.94 (80)
$[CrFe_2(MeL)_6]ClO_4 \cdot 2H_2O$	*g*	*h*	0.59 (100), 0.43 (100)
$[Fe_3(MeL)_6]ClO_4 \cdot 2H_2O$	0.01 (150)	0.98 (−0.27)	0.81 (80), 1.01 (60)
$[Fe_3(PhL)_6]ClO_4$	−0.01 (140)	1.05 (−0.28)	0.68 (60), 0.88 (60)
$NaFe(MeL)_3 \cdot H_2O$	0.30 (180)	0.97 (0.60)	1.33[j]
$NaFe(PhL)_3 \cdot H_2O$	0.38 (200)	1.02 (0.68)	1.20[j]

[a] Meanings of the symbols used are the same as in the text. [b] Supporting electrolyte is TEAP (0.1 M); working electrode is platinum. [c] Cyclic voltammetric data in dichloromethane; scan rate 50 mV s^{-1}. [d] Constant-potential coulometric data. [e] $n = Q/Q'$, where Q is the observed coulomb count and Q' is the calculated coulomb count for 1e transfer; E is the constant potential at which electrolysis is performed. [f] Cyclic voltammetric data in acetonitrile; scan rate 50 mV s^{-1}. [g] No observable central metal-based redox response. [h] Measurement is not made. [i] Due to insufficient solubility in acetonitrile, measurement is not made. [j] Cathodic peak potential.

E. Redox Behavior. The cyclic voltammetric responses pertaining to the central metal atom and the terminal $Fe(RL)_3^-$ moieties are best observed in dichloromethane and acetonitrile, respectively (platinum electrode). Results are in Table V and Figures 5 and 6. All potentials are referenced to the saturated calomel electrode (SCE). The formal potential $E°_{298}$ is taken as the average of anodic and cathodic peak potentials (E_{pa} and E_{pc}). The separation $E_{pa} - E_{pc}$ is ΔE_p.

(a) Metal Oxidation within $Fe(RL)_3^-$. Free $Fe(RL)_3^-$ (as in Na^+ and Ph_4As^+ salts) shows a quasi-reversible[27] response due to the process (5). In $MFe_2(RL)_6$ no response corresponding to

$$Fe^{III}(RL)_3 + e^- \rightleftharpoons Fe^{II}(RL)_3^- \quad (5)$$

couple 5 is observed up to 1 V.[28] The $MFe_2(RL)_6^+$ complexes behave similarly. It is expected that, on intimate binding of metal cations to $Fe(RL)_3^-$, the oxidation of the iron(II) center would become less favorable, resulting in higher $E°_{298}$ values. In practice, metal oxidation becomes unobservable.[28]

(b) The $M^{III}O_6/M^{II}O_6$ Couple. When the central metal ion is oxidizable below 1 V, redox response due to electron transfer within the MO_6 core (eq 6) is observed (Figure 5) as in the cases of $MFe_2(RL)_6$ (M = Mn,[29] Fe, Co). Knowledge of the formal

$$M^{III}Fe_2(RL)_6^+ + e^- \rightleftharpoons M^{II}Fe_2(RL)_6 \quad (6)$$

potentials (Table V) of couple 6 in the cases of M = Mn, Fe, and Co allows us to estimate the potential for the M = Ni case to be ~1.3 V by using a linear extrapolation procedure.[30,31] Ligand oxidation[28] precludes observation of the predicted nickel(III)–nickel(II) couple. The one-electron stoichiometry of couples 5 and 6 is based on current height and constant-potential coulometric data[32] (Table V).

Table VI. Crystal Data for $NiFe_2(MeL)_6 \cdot CH_2Cl_2$

formula	$NiFe_2Cl_2O_6N_{18}C_{49}H_{50}$
fw	1228.4
space group	$P2_1/n$
systematic absences	$(0k0)$, $k = 2n + 1$; $(h0l)$, $h + l = 2n + 1$
a, Å	29.607 (18)
b, Å	19.732 (11)
c, Å	10.040 (4)
β, deg	90.53 (4)
V, Å^3	5865 (5)
Z	4
d_{calcd}, g/cm^3	1.391
cryst size, mm	0.65 × 0.40 × 0.01
μ(Mo Kα), cm^{-1}	9.72
data collecn instrument	Syntex P$\bar{1}$
radiation (monochromated in incident beam)	Mo Kα (λ_α = 0.71073 Å)
orientation reflcns: no., range (2θ)	15, 19 < 2θ < 28°
scan method	ω scans
data collecn range, 2θ, deg	4.0 ≤ 2θ ≤ 50.0
no. of unique data, total with $F_o^2 \geq 3\sigma(F_o^2)$	2554, 1886
no. of parameters refined	370
transmission factors: max, min	calcd 0.99, 0.48; obsd 1.00, 0.82
R^a	0.0734
R_w^b	0.0933
quality-of-fit indicator[c]	1.810
largest shift/esd, final cycle	0.20
largest peak, e/Å^3	0.85

[a] $R = \sum||F_o| - |F_c||/\sum|F_o|$. [b] $R_w = [\sum w(|F_o| - |F_c|)^2/\sum w|F_o|^2]^{1/2}$; $w = 1/\sigma^2(|F_o|)$. [c] Quality of fit = $[\sum w(|F_o| - |F_c|)^2/(N_{observns} - N_{parameters})]^{1/2}$.

(c) Ligand Reduction. Sodium and tetraphenyl arsonium salts of $Fe(MeL)_3^-$ show a cathodic peak at −1.33 V. The corresponding anodic response is ill-developed. In $MFe_2(MeL)_6$[33] a pair of overlapping reversible to quasi-reversible (ΔE_p = 60–120 mV) 1e couples occur near −0.8 and −1.0 V. In the case of $CrFe_2(MeL)_6^+$ the corresponding couples occur at much higher potentials (Figure 6 and Table V). The observation of the pair is a *diagnostic feature* of the trinucleation.[34]

It has been recognized[9,11,35] that metal arylazo oximates display reductive responses on the negative side of the SCE due to electron transfer to the azo function (eq 7). The observed reduction of

$$-N{=}N- + e^- \rightleftharpoons [-N\dot{-}\dot{N}-]^- \quad (7)$$

$$Fe^{II}(MeL)_3^- + e^- \rightleftharpoons Fe^{II}(MeL)_3^{2-} \quad (8)$$

$Fe(MeL)_3^-$ is accordingly assigned to ligand reduction (eq 8). The corresponding reduction in isoelectronic (but meridional[8]) $Co(MeL)_3$ is quasi-reversible and occurs[36] at a higher potential (−0.75 V) as expected (iron(II) vs. cobalt(III)). The lack of a good anodic response for the iron complex is probably due to the instability and consequent decomposition of the binegative reduced species. This species is expected to get stabilized in the presence of closely bound cations. This indeed happens in the trinuclear complexes, where the cathodic and anodic responses are of equal height. The invariable occurrence of a pair of redox couples here can be

(27) The ΔE_p (150–200 mV) values in dichloromethane are higher than those in acetonitrile (80–120 mV).[1]
(28) Above 1 V irreversible oxidation phenomena are observed presumably due to ligand oxidation.[1]
(29) In the case of $MnFe_2(PhL)_6$ a second quasi-reversible oxidation with current height appropriate for a 1e process is observed at $E°_{298}$ = 1.21 V (ΔE_p = 120 mV). Whether this is a Mn(IV)/Mn(III) couple has not been ascertained since ligand oxidation can also occur at this potential.
(30) This procedure[31] consists of a linear correlation and extrapolation of the known formal potentials of the $M(bpyO_2)_3^{3+}/M(bpyO_2)_3^{2+}$ couple (M = Mn (+0.79 V), Fe (+0.13 V), Co (+0.87 V), Ni (+1.47 V); $bpyO_2$ = 2,2′-bipyridine 1,1′-dioxide) with the formal potentials of couple 6. We note that the $(bpyO_2)_3$ chelates have MO_6 octahedra.
(31) Bhattacharya, S.; Mukherjee, R. N.; Chakravorty, A., unpublished results.
(32) The coulometrically oxidized solutions undergo partial decompositions to afford $Fe^{III}(RL)_3$, which in turn furnishes[1] $Fe_3(RL)_6^+$. These rate processes are under scrutiny with the help of cyclic voltammetry and EPR spectroscopy. The decomposition is more pronounced in R = Ph species than in R = Me species. The M = Co complexes decompose to a greater extent than the M = Mn complexes.
(33) The $MFe_2(PhL)_6$ complexes are insufficiently soluble in acetonitrile for accurate electrochemical work.
(34) As one goes to potentials more negative to the pair, other reductive responses, often attended by high currents, are observed. Such responses are not described in the present work.
(35) Chakravarty, A. R.; Chakravorty, A. *J. Chem. Soc., Dalton Trans.* **1982**, 615.
(36) Ghosh, P.; Chakravorty, A., unpublished results.

Table VII. Atomic Positional Parameters and Isotropic (or Isotropic-Equivalent) Thermal Parameters and Their Estimated Standard Deviations for $NiFe_2(MeL)_6 \cdot CH_2Cl_2$[a]

atom	x	y	z	B, Å²	atom	x	y	z	B, Å²
Ni	0.0637 (1)	0.1543 (2)	0.1785 (3)	3.18 (7)	C(11)	0.1563 (7)	−0.110 (1)	0.382 (2)	2.8 (5)*
Fe(1)	0.1485 (1)	0.0397 (2)	0.2657 (3)	3.06 (8)	C(12)	0.1596 (8)	−0.143 (1)	0.261 (2)	4.2 (6)*
Fe(2)	−0.0227 (1)	0.2671 (2)	0.1006 (4)	2.99 (8)	C(13)	0.1774 (8)	−0.211 (1)	0.270 (3)	4.8 (7)*
Cl(1)	0.5536 (6)	0.242 (1)	0.187 (2)	11.0 (5)*	C(14)	0.1889 (9)	−0.240 (1)	0.393 (3)	5.9 (7)*
Cl(2)	0.5592 (9)	0.138 (1)	0.008 (3)	17.6 (9)*	C(15)	0.1847 (9)	−0.203 (2)	0.505 (3)	5.7 (7)*
Cl(3)	0.210 (1)	0.174 (2)	0.888 (3)	13.0 (9)*	C(16)	0.1683 (8)	−0.135 (1)	0.508 (3)	4.8 (7)*
Cl(4)	0.175 (1)	0.286 (2)	0.790 (3)	15 (1)*	C(17)	0.1866 (8)	0.169 (1)	0.288 (3)	5.0 (7)*
O(1)	0.0637 (4)	0.0539 (8)	0.125 (1)	3.8 (4)	C(18)	0.1930 (8)	0.244 (1)	0.267 (3)	5.3 (7)*
O(2)	0.0829 (5)	0.1339 (8)	0.371 (1)	3.9 (4)	C(19)	0.2187 (8)	0.032 (1)	0.496 (2)	4.6 (6)*
O(3)	0.1310 (5)	0.1635 (8)	0.124 (1)	3.5 (4)	C(20)	0.2474 (9)	−0.019 (2)	0.463 (3)	6.3 (8)*
O(4)	−0.0015 (5)	0.1437 (8)	0.236 (1)	3.4 (4)	C(21)	0.267 (1)	−0.058 (2)	0.576 (3)	7.6 (9)*
O(5)	0.0426 (5)	0.1795 (8)	−0.013 (1)	3.5 (4)	C(22)	0.255 (1)	−0.041 (2)	0.706 (3)	7.5 (8)*
O(6)	0.0639 (4)	0.2547 (7)	0.231 (1)	2.8 (4)	C(23)	0.227 (1)	0.012 (2)	0.731 (3)	6.8 (8)*
N(1)	0.1844 (6)	−0.003 (1)	0.130 (2)	3.1 (4)*	C(24)	0.2015 (9)	0.054 (2)	0.622 (3)	6.3 (8)*
N(2)	0.1617 (6)	−0.022 (1)	0.025 (2)	3.5 (5)*	C(25)	−0.0299 (7)	0.161 (1)	−0.077 (2)	3.1 (5)*
N(3)	0.1040 (5)	0.0278 (9)	0.125 (2)	2.6 (4)*	C(26)	−0.0190 (8)	0.101 (1)	−0.166 (2)	4.6 (6)*
N(4)	0.1372 (6)	−0.040 (1)	0.376 (2)	3.5 (4)*	C(27)	−0.1235 (7)	0.250 (1)	0.045 (2)	3.1 (5)*
N(5)	0.1102 (6)	−0.029 (1)	0.477 (2)	3.9 (5)*	C(28)	−0.1397 (7)	0.316 (1)	0.013 (2)	3.6 (6)*
N(6)	0.1025 (5)	0.0734 (9)	0.378 (2)	2.8 (4)*	C(29)	−0.1844 (8)	0.332 (1)	0.029 (3)	4.7 (6)*
N(7)	0.1972 (6)	0.067 (1)	0.380 (2)	4.2 (5)*	C(30)	−0.2136 (8)	0.286 (1)	0.085 (2)	4.5 (6)*
N(8)	0.2078 (6)	0.130 (1)	0.380 (2)	4.2 (5)*	C(31)	−0.1978 (8)	0.217 (1)	0.121 (3)	4.7 (6)*
N(9)	0.1570 (6)	0.132 (1)	0.211 (2)	3.6 (4)*	C(32)	−0.1526 (8)	0.202 (1)	0.097 (2)	4.2 (6)*
N(10)	−0.0773 (5)	0.234 (1)	0.020 (2)	2.8 (4)*	C(33)	−0.0478 (7)	0.217 (1)	0.345 (2)	3.7 (6)*
N(11)	−0.0746 (6)	0.183 (1)	−0.059 (2)	3.6 (5)*	C(34)	−0.0474 (8)	0.175 (1)	0.469 (3)	5.0 (7)*
N(12)	0.0009 (5)	0.1988 (9)	−0.013 (2)	2.0 (4)*	C(35)	−0.0791 (8)	0.378 (1)	0.251 (2)	4.0 (6)*
N(13)	−0.0568 (5)	0.3127 (9)	0.246 (2)	2.6 (4)*	C(36)	−0.1229 (8)	0.383 (1)	0.293 (2)	4.5 (6)*
N(14)	−0.0660 (6)	0.278 (1)	0.349 (2)	3.4 (4)*	C(37)	−0.1431 (8)	0.448 (1)	0.301 (3)	4.9 (6)*
N(15)	−0.0237 (6)	0.200 (1)	0.242 (2)	3.5 (4)*	C(38)	−0.1191 (9)	0.509 (2)	0.265 (3)	6.0 (7)*
N(16)	−0.0116 (5)	0.3440 (9)	−0.015 (2)	2.1 (4)*	C(39)	−0.0748 (9)	0.499 (1)	0.218 (3)	5.2 (7)*
N(17)	0.0269 (6)	0.374 (1)	0.004 (2)	3.3 (4)*	C(40)	−0.0536 (9)	0.434 (1)	0.209 (3)	5.5 (7)*
N(18)	0.0369 (6)	0.2906 (9)	0.156 (2)	3.0 (4)*	C(41)	0.0531 (8)	0.343 (1)	0.098 (2)	4.2 (6)*
C(1)	0.1175 (7)	−0.008 (1)	0.020 (2)	3.2 (5)*	C(42)	0.1022 (8)	0.369 (1)	0.117 (2)	4.3 (6)*
C(2)	0.0898 (7)	−0.015 (1)	−0.099 (2)	2.6 (5)*	C(43)	−0.0340 (7)	0.372 (1)	−0.129 (2)	3.0 (5)*
C(3)	0.2328 (7)	−0.016 (1)	0.118 (2)	3.0 (5)*	C(44)	−0.0372 (8)	0.439 (1)	−0.139 (2)	4.5 (6)*
C(4)	0.2480 (8)	−0.078 (1)	0.087 (3)	5.2 (7)*	C(45)	−0.0586 (9)	0.467 (2)	−0.258 (3)	6.8 (8)*
C(5)	0.2969 (8)	−0.087 (1)	0.080 (3)	4.8 (6)*	C(46)	−0.0734 (8)	0.424 (1)	−0.358 (2)	4.1 (6)*
C(6)	0.3248 (9)	−0.031 (1)	0.109 (3)	5.8 (7)*	C(47)	−0.0726 (8)	0.352 (1)	−0.343 (3)	4.8 (6)*
C(7)	0.3079 (9)	0.034 (1)	0.138 (3)	5.7 (7)*	C(48)	−0.0524 (8)	0.325 (1)	−0.222 (3)	4.9 (7)*
C(8)	0.2596 (8)	0.042 (1)	0.143 (2)	4.7 (6)*	C(49)	0.564 (2)	0.215 (4)	0.035 (7)	11 (2)*
C(9)	0.0897 (7)	0.033 (1)	0.473 (2)	3.4 (5)*	C(50)	0.151 (3)	0.210 (5)	0.825 (9)	10 (3)*
C(10)	0.0537 (7)	0.051 (1)	0.576 (2)	3.6 (6)*					

[a] Starred atoms were refined isotropically. Anisotropically refined atoms are given in the form of the isotropic equivalent thermal parameter defined as $^4/_3[a^2\beta_{11} + b^2\beta_{22} + c^2\beta_{33} + ab(\cos\gamma)\beta_{12} + ac(\cos\beta)\beta_{13} + bc(\cos\alpha)\beta_{23}]$.

rationalized in terms of successive electron transfers to the two bound $Fe(MeL)_3^-$ moieties. The positive shift of the potentials in going from $M^{II}Fe_2(MeL)_6$ to $Cr^{III}Fe_2(MeL)_6^+$ is understandable in view of the increased positive charge of the central metal atom.[37] The $Fe_3(MeL)_6^+$ species provides an interesting situation. Here the central metal atom is iron(III), but below ~0.0 V it is converted[1] to the iron(II) analogue $Fe_3(MeL)_6$. The observed ligand reduction potentials (Table V) are therefore close to those of $M^{II}Fe_2(MeL)_6$.

F. Concluding Remarks. The ability of six arylazo oxime molecules to afford trinuclear complexes goes beyond the specific complex **1** reported earlier.[1] It now emerges that the central metal atom can be either a bivalent (Mn, Co, Ni, Zn)[38] or a trivalent (Fe,[1] Cr) 3d ion. Good X-ray-quality crystals of the trinuclear complexes are difficult to get in most cases. However, EPR and electrochemical techniques afford very useful diagnostic tools for characterizing trinucleation. Thus the small distortion of the NiO_6 octahedron in X-ray-characterized $NiFe_2(MeL)_6 \cdot CH_2Cl_2$ is neatly reflected in the EPR spectrum of the manganese(II) congener doped into the nickel(II) lattice.

The real scope of trinucleation affording $MFe_2(RL)_6^{(z-2)+}$ (z = 2, 3) is indeed very widespread. The alkaline-earth (z = 2) and lanthanide (z = 3) complexes can be synthesized with ease and will be described in subsequent publications. The more challenging task is to replace iron(II) in $Fe(RL)_3^-$ by other metal ions yet affording the trinuclear configuration. We have been able to achieve this in the cases of osmium(II) and manganese(II). This interesting chemistry will be reported elsewhere.

Experimental Section

Materials. Arylazo oximes,[39] salts of[1] $Fe_3(RL)_6^+$, and $NaFe(RL)_3 \cdot H_2O$[1,7] were prepared by using reported methods. Hydrated transition-metal perchlorates were prepared by treating the corresponding metal carbonates or hydroxides with 70% aqueous perchloric acid followed by crystallization. The purification of solvents and supporting electrolyte (tetraethylammonium perchlorate, TEAP) for electrochemical work was done as before.[16] All other chemicals and organic solvents used were of reagent grade and were used without further purification.

Measurements. Electronic spectra were measured on Cary 17D and Hitachi 330 spectrophotometers. The Gaussian fitting of optical bands was done by using a standard procedure[40] with frequency as the spectral ordinate. The results were recast on the wavelength scale (Figure 3). IR spectra (KBr disk) were recorded with Beckman IR-20A and Perkin-Elmer 783 spectrophotometers. For X-band EPR spectra a Varian E-109C spectrometer fitted with a quartz Dewar for measurements at 77 K (liquid dinitrogen) was used. The EPR spectra were calibrated with

(37) By using a linear extrapolation procedure similar to that used[30] for $NiFe_2(MeL)_6$, the formal potential of the $Cr^{III}O_6/Cr^{II}O_6$ couple (couple 6) is estimated to be −0.9 V. Thus ligand reduction precedes reduction of the central chromium ion, and this in turn would make the latter reduction even more difficult. In practice we have not been able to observe couple 6 here.

(38) The copper(II) complexes, $CuFe_2(RL)_6$, have also been synthesized. Their EPR spectra are however complex apparently due to distortion and await analysis.

(39) Kalia, K. C.; Chakravorty, A. *J. Org. Chem.* **1970**, *35*, 2231.
(40) Barker, B. E.; Fox, M. F. *Chem. Soc. Rev.* **1980**, *9*, 143.

the help of DPPH (g = 2.0037). Magnetic susceptibility was measured with a PAR vibrating-sample magnetometer (Model 155) fitted with a Walker Scientific magnet (Model L75FBAL). Solution electrical conductivity was measured with a Philips PR 9500 bridge with a solute concentration of $\sim 10^{-3}$ M. Electrochemical measurements were done by using a PAR Model 370-4 electrochemistry system incorporating the following equipment: 174A, polarographic analyzer; 175, universal programmer; RE 0074, XY recorder; 173, potentiostat; 179, digital coulometer; 377A, cell system. All experiments were performed under dry and purified dinitrogen atmospheres. A planar Beckman Model 39273 platinum-inlay working electrode, a platinum-wire auxiliary electrode, and an aqueous saturated calomel reference electrode (SCE) were used in the three-electrode measurements. A platinum-wire-gauze working electrode was used in coulometric experiments. All electrochemical data were collected at 298 K and are uncorrected for junction potentials.

Preparation of Complexes. All compounds were prepared with use of similar methods. Details are therefore given for a representative case.

Bis[tris((phenylazo)acetaldoximato)ferrato(II)]nickel(II) Dihydrate, $[NiFe_2(MeL)_6]\cdot 2H_2O$. To a solution of $NaFe(MeL)_3\cdot H_2O$ (0.39 g, 0.67 mmol) in ethanol (20 mL) was added 0.13 g (0.36 mmol) of $Ni(ClO_4)_2\cdot 6H_2O$, and the mixture was heated to reflux for 1 h. It was then cooled to 273 K, and a black crystalline solid separated after 6 h. This was collected by filtration, washed thoroughly with water (273 K), and dried under vacuum over P_4O_{10}; yield 0.29 g (74%). Anal. Calcd for $NiFe_2C_{48}H_{52}N_{18}O_8$: Ni, 4.98; Fe, 9.48; C, 48.88; H, 4.41; N, 21.38. Found: Ni, 5.01; Fe, 9.66; C, 49.02; H, 4.26; N, 21.43.

Dark square crystals of composition $NiFe_2(MeL)_6\cdot CH_2Cl_2$ resulted by slow diffusion of hexane (25 mL) into a dichloromethane solution (25 mL) of $NiFe_2(MeL)_6\cdot 2H_2O$ (7 mg) and were used for the X-ray work.

The complex $NiFe_2(PhL)_6$ (yield 80%) was prepared by using the procedure as described above except that HPhL was used in place of HMeL. Anal. Calcd for $NiFe_2C_{78}H_{60}N_{18}O_6$: Ni, 3.88; Fe, 7.38; C, 61.81; H, 3.96; N, 16.64. Found: Ni, 3.89; Fe, 7.47; C, 62.02; H, 3.90; N, 16.59.

Analytical data for other complexes prepared similarly are as follows. Anal. Calcd for $[CrFe_2(MeL)_6]ClO_4\cdot 2H_2O$, $CrFe_2C_{48}H_{52}N_{18}O_{14}Cl$: Cr, 4.09; Fe, 8.79; C, 45.31; H, 4.09; N, 19.82; Cl, 2.79. Found: Cr, 4.31; Fe, 9.02; C, 45.27; H, 4.38; N, 19.75; Cl, 3.30. Calcd for $MnFe_2(MeL)_6\cdot 2H_2O$, $MnFe_2C_{48}H_{52}N_{18}O_8$: Mn, 4.68; Fe, 9.51; C, 49.04; H, 4.43; N, 21.45. Found: Mn, 4.82; Fe, 9.71; C, 49.39; H, 4.53; N, 21.62. Calcd for $MnFe_2(PhL)_6$, $MnFe_2C_{78}H_{60}N_{18}O_6$: Mn, 3.64; Fe, 7.39; C, 61.96; H, 3.97; N, 16.68. Found: Mn, 3.41; Fe, 7.50; C, 61.73; H, 4.18; N, 16.42. Calcd for $CoFe_2(MeL)_6\cdot 2H_2O$, $CoFe_2C_{48}H_{52}N_{18}O_8$: Fe, 9.48; C, 48.87; H, 4.41; N, 21.38. Found: Fe, 9.62; C, 48.79; H, 4.53; N, 21.89. Calcd for $CoFe_2(PhL)_6$, $CoFe_2C_{78}H_{60}N_{18}O_6$: Fe, 7.37; C, 61.80; H, 3.96; N, 16.64. Found: Fe, 7.47; C, 61.45; H, 3.95; N, 16.33. Calcd for $ZnFe_2(MeL)_6\cdot 2H_2O$, $ZnFe_2C_{48}H_{52}N_{18}O_8$: Fe, 9.43; C, 48.60; H, 4.39; N, 21.26. Found: Fe, 9.40; C, 48.82; H, 4.10; N, 21.34. Calcd for $ZnFe_2(PhL)_6$, $ZnFe_2C_{78}H_{60}N_{18}O_6$: Fe, 7.34; C, 61.54; H, 3.94; N, 16.57. Found: Fe, 7.41; C, 62.10; H, 4.01; N, 16.42.

Crystal Structure Determination: Data Collection and Reduction. A thin crystalline plate was mounted at the end of a glass fiber and covered with a thin layer of epoxy. All geometrical and intensity data were taken from this crystal, by an automated four-circle diffractometer. The unit-cell determination and data collection were conducted by standard procedures described previously.[41] Crystal data are summarized in Table VI. The lattice dimensions and Laue class ($2/m$) were verified by axial photography.

An ω range of 1.02° was used in scanning each of 2950 possible data points with a variable scan speed between 1.0 and 24.0°/min. Three check reflections, monitored at regular intervals, did not vary appreciably in intensity during the 108 h of X-ray exposure time.

Data were reduced by standard procedures.[42] An empirical absorption correction[43] was based on azimuthal scans of 7 reflections with diffractometer angle χ near 90°. The number of unique data (1886) represents less than the full amount of data theoretically accessible; the relative weakness of the diffraction pattern was caused by the thinness of the crystal.

Systematic absences uniquely established the space group as $P2_1/n$.

Structure Solution and Refinement. The positions of the three unique metal atoms were derived from a Patterson map, and the remainder of the structure was developed and refined in a series of alternating least-squares analyses and difference Fourier maps. The source of atomic scattering factors and the function minimized were as described elsewhere.[41,44]

Two molecules of CH_2Cl_2 were found in the lattice. In order to achieve acceptable thermal parameters for the atoms in these groups, it was necessary to use a model in which the sites were partially occupied. (A contact distance of ca. 3.3 Å between atom Cl(1) of one of the molecules and atom C(50) of the other also points to partial occupancy.) In the last stages of refinement, fixed site occupation factors of 0.60 and 0.40 were assigned to the CH_2Cl_2 molecules containing atoms C(49) and C(50), respectively.

In the final refinement positional parameters were refined for 81 atoms. Nine atoms were refined with anisotropic thermal parameters, and the remainder were treated as isotropic. In all, 370 variable parameters were fitted to 1886 data. The refinement converged (largest parameter shift/esd 0.20) with final residuals (defined and summarized in Table VI) of R = 0.0734, R_w = 0.0933, and quality of fit 1.810. The largest peak on a difference map following the refinement had a density of 0.85 e/Å^3. The refinement did not suffer from any noticeable correlation effects, and there was no significant variation in R factor as a function of $(\sin\theta)/\lambda$, as a function of the magnitude of $|F_o|$, or as a function of parity group. Atomic positional parameters and isotropic or isotropic-equivalent thermal parameters are listed in Table VII.

Acknowledgment. Our very special thanks are due to Professor F. A. Cotton for being extremely helpful in many ways. Financial help received from the Department of Science and Technology and Council of Scientific and Industrial Research, New Delhi, India, is gratefully acknowledged. We are also thankful to Dr. A. R. Chakravarty for doing some preliminary experiments.

Registry No. $NiFe_2(MeL)_6\cdot CH_2Cl_2$, 99617-80-8; $MnFe_2(MeL)_6$, 99617-81-9; $NiFe_2(PhL)_6$, 99617-82-0; $CoFe_2(PhL)_6$, 99617-83-1; $CoFe_2(MeL)_6$, 99617-84-2; $MnFe_2(PhL)_6$, 99617-85-3; $ZnFe_2(MeL)_6$, 99617-86-4; $ZnFe_2(PhL)_6$, 99617-87-5; $CrFe_2(MeL)_6ClO_4$, 99617-89-7; Mn^{2+}, 16397-91-4; $NaFe(MeL)_3$, 70198-84-4; $NaFe(PhL)_3$, 40557-43-5.

Supplementary Material Available: Listings of bond distances (Table VIII), bond angles (Table IX), least-squares planes and dihedral angles (Table X), torsion angles (Table XI), anisotropic thermal parameters (Table XII), observed and calculated structure factors (Table XIII), and UV–vis absorption maxima and intensities for all complexes (Table XIV) and an ORTEP drawing of the entire complex $NiFe_2(MeL)_6$ (Figure 7) (32 pages). Ordering information is given on any current masthead page.

(41) Cotton, F. A.; Frenz, B. A.; Deganello, G.; Shaver, A. *J. Organomet. Chem.* **1973**, *50*, 227.
(42) Crystallographic calculations were done on a VAX-11/780 computer, with programs from the Enraf-Nonius Package, VAXSDP.
(43) North, A. C. T.; Phillips, D. C.; Mathews, F. S. *Acta Crystallogr., Sect. A: Cryst. Phys., Diffr., Theor. Gen. Crystallogr.* **1968**, *A24*, 351.
(44) Cotton, F. A.; Extine, M.; Gage, L. D. *Inorg. Chem.* **1978**, *17*, 172.